Coupled High-Strength Window and Mullion Model Validation

Carrie Davis, P.E.
Protection Engineering Consultants, USA

Kirk Marchand, P.E.
Protection Engineering Consultants, USA

Edward Conrath, P.E.
Protection Engineering Consultants, USA

Ryan Alberson, P.E.
Independent Consultant, USA

Abstract
Glazing in storefront and curtainwall configurations are increasingly used in areas subjected to blast load. Current design approaches typically use single degree of freedom (SDOF) methods to analyse the performance of both the window glazing and mullions. The flexural resistance and mass of each component must be identified to solve the SDOF representation. Then, the resistance curve is calculated based on span, support conditions, cross sectional stiffness, assumed deformed shape, and a failure criterion. This paper addresses the latter two critical parameters.

Dynamic verification of deformed shape is difficult to assess through testing and has historically been calculated through analytical and numerical methods. However, new measurement methods provide high resolution, high speed deformation measurements through the use of Digital Image Correlation, which is a stereoscopic camera setup capable of measuring three dimensional deflections of both the window glazing and mullions simultaneously. This allows analysis of deformed shape and the interaction between the glazing and mullions. The failure point for the resistance curve was determined by modifying the Glass Failure Prediction Model (basis for ASTM E1300) to handle high-strength glass. Together these models were used to validate SDOF and finite element models used in industry for storefronts comprised of high-strength glass.

1. Introduction
Protection Engineering Consultants (PEC) was engaged by the Air Force Research Laboratory (AFRL) to evaluate the performance of window systems consisting of PPG's Herculite® XP glass installed in commercial grade frames and storefront systems such that a fast running model could be developed to be used as a design tool enabling engineers to specify Herculite® XP glass. Herculite® XP glass is a high strength glass technology developed by PPG Industries with a residual stress about twice that of commercially produced fully tempered (FT) glass. The research program included quasi-static tests of Herculite® XP glass at PEC, shock tube tests of punched windows (insulating glass units (IGUs) with commercial window frames containing Herculite® XP glass) at ABS Consulting, and two full-scale blast tests at AFRL on IGUs containing Herculite® XP glass in punched window and storefront configurations using typical commercial window frames and storefront systems [1].

This paper presents developments in the application of the failure prediction model based on experimental observations of deformed shape and glass fracture.

2. Glass Failure Criterion History, Improvement and Implementation
The AFRL test program was conceived to validate a model capable of predicting glass failure for both static and dynamic loads. The Glass Failure Prediction Model (GFPM) developed by Beason and Morgan [2] was chosen for its incorporation of load rate, empirical flaw probability distribution (validated), and because it is the basis for the industry standard ASTM E1300 design methodology [3,4]. However, the GFPM was originally developed to only accommodate annealed (AN) glass and required modifications to address the increased strength of Herculite® XP glass.

To summarize the basic premise, the GFPM uses a finite difference model after Vallabahn and Wang [5] to correlate the lateral pressure on a given piece of glass to its stress distribution. The stress is then modified to account for load duration and biaxiality, which is referenced as the equivalent stress. The equivalent stress is incorporated into a Weibull distribution where empirical flaw parameters (m, k) define the shape of the Weibull distribution and relate equivalent stress to the probability of failure. Two methods of GFPM modifications are presented below followed by a description of the test program and data used for validation.

2.1 SBEDS-W GFPM Methodology
SBEDS-W (Single degree of freedom Blast Effects Design Spreadsheet for Windows) [6] uses the GFPM to predict glass failure for SDOF analysis. Specifically, SBEDS-W uses the method presented in ASTM E1300 Appendix X3. Use of the stress distribution factor, J, eliminates the need to explicitly map the relationship between lateral load and stress in the glass. However, the stress distribution factor is based on testing of AN glass only. To accommodate the increased strength of Herculite® XP glass, a strength

multiplier was added to the model which has a similar effect as altering the *k* parameter of the Weibull distribution found in the GFPM. Due to this modification, the *k* parameter is fixed at a value of $2.86x10^{-53}$ in SBEDS-W. Therefore, the *m* parameter is the only variable used to calibrate differing strengths of glass (in addition to the embedded strength factor). This parameter was established through both static and dynamic testing.

2.2 An Extended GFPM Method

To identify the GFPM flaw parameters for Herculite® XP glass, PEC used an implicit FEA analysis by LS-DYNA to map stress to lateral load on the glass. This supplants the original finite difference model found in the GFPM, but accomplishes the same task. Results were validated for AN glass using static test data to verify model accuracy. Additionally, the deflection data from this model verified the polynomial method for calculating deflection of the midpoint presented in ASTM E1300 Appendix X2. This approach in modifying the GFPM differs from the approach using the GFPM implementation in SBEDS-W, but both yield conservative results when compared to blast test data.

2.3 Modified GFPM Model Comparison

Figures 1 and 2 show the cumulative Weibull distribution (failure probability) using both the original and adjusted set of flaw parameters plotted against the lateral pressure on the glass. Both models of the modified GFPM are shown for comparison (SBEDS-W and RCSS).

The SBEDS-W model represents the approach used by PEC over the course of this project and uses an *m* value of 6.55 while *k* is treated as a constant (k=2.86e^{-53} N^{-7}m^{12}). The RCSS version was run with both original flaw parameters (m=7, k=2.86e^{-53} N^{-7}m^{12}) and adjusted values (m=3, k=1.56e^{-23} N^{-3}m^{4}). To adjust the Weibull distribution parameters, several pairs of flaw parameters were plotted against test data until the cumulative distribution encompassed most test values (minimizing the number of test values in the tails of the distribution curve). This adjustment proved to be robust across multiple sizes, thicknesses, and load durations. Also, notice that that SBEDS-W model is consistently conservative and tuned for better correlation on dynamic test results (compared to the quasi-static tests).

The resistance of the glass was not directly measured in dynamic testing (shock tube and blast testing) as material resistances are extremely difficult to measure directly when combined with inertial resistances. Resistance was thus inferred from measured deflection and known mass distribution based on deformed shape. The deflection was measured over time through the use of a laser gauge and the time of failure was determined from high speed video. The resistance curve relates the deflection to the lateral pressure and the time of failure was used to identify the maximum deflection and subsequent pressure (resistance) on the glass.

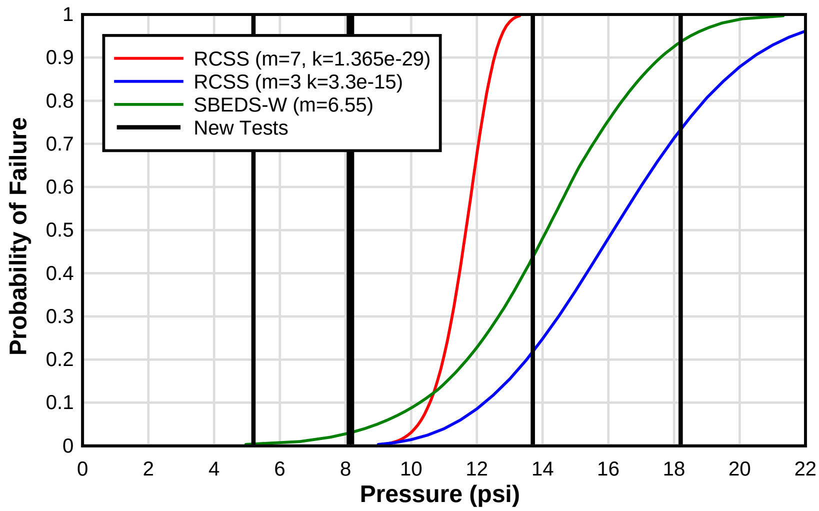

Figure 1. Dynamic Test Validation (152.4cm x 76.2cm x 5.6mm Herculite® XP glass)

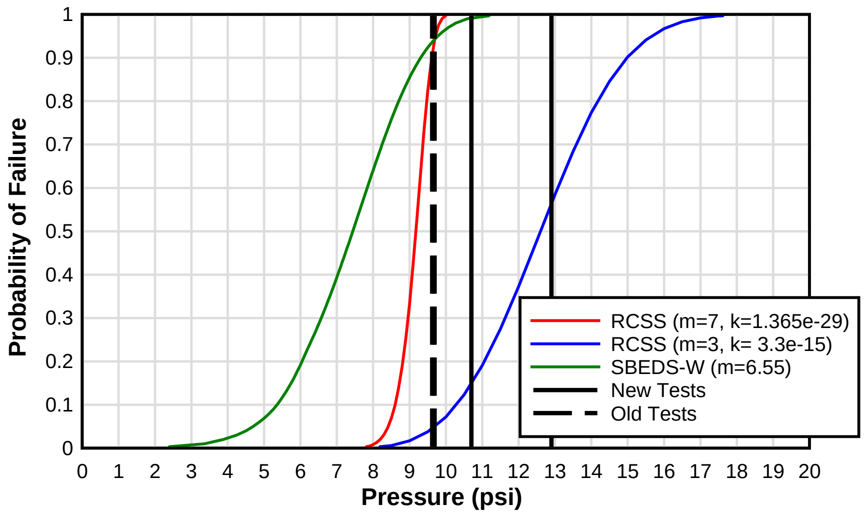

Figure 2. Static Test Validation (152.4cm x 76.2cm x 5.6mm Herculite® XP glass)

Figures 1 and 2 show good results from both models based on conservative predictions from the probability distribution. The RCSS GFPM has better handling of load duration than the SBEDS-W GFPM as evidenced by a better probability envelope for both static and dynamic testing. However, SBEDS-W is only used for dynamic events and thus the embedded GFPM method is specifically calibrated for such events and performs well based on test results plotted against the probability distribution. For longer duration loads, the SBEDS-W methodology will be conservative.

3. Testing and Data Collection

3.1 Shock Tube Testing.

Shock tube testing provided an abundance of data with regard to deformed shape, crack propagation, glass deflection at failure, and polyvinyl butyral (PVB) bite considerations. Deflection of the glazing was measured via laser gages. High speed cameras were used to capture crack propagation, which was used to assess glass break timing and to correlate displacement at time of failure. This was used to improve the predictive capabilities of the GFPM found in SBEDS-W. Additionally, stereo cameras were set-up to capture high speed video for use with DIC software to analyse the deformed shape of the glazing, which is further discussed in section 4.

The initial monolithic glass tests were performed to investigate rate effects included in the GFPM model. Layups tested are summarized in Table 1. Shock tube test results and predictions using an *m* of 6.4 in SBEDS-W are summarized in Table 2. SBEDS-W predicted slightly higher deflections and resistances to first crack than observed in the tests. Additionally, the break point of glass was predicted correctly 57% of the time based on flaw parameters determined from static testing. Using the dynamic test data, *m* was adjusted to 6.55 to account for these differences which were most likely due to rate effects and assumed deformed shape. The effect of inertia is seen in Figure 3 where the observed test data initially lags behind the idealized window response calculated by SDOF analysis in SBEDS-W. This inertial effect is discussed further in section 4.

Table 1. Shock Tube Tests Glass Layup Types

Glass Layup Type	No. of Samples	Nominal Thickness (in)			Frame Type
		Outer Lite	Air Gap	Inner Lite*	
1	4	3/16	1/2	1/4 laminate (0.060 PVB)	aluminum
2	3	1/4	1/2	5/16 laminate (0.060 PVB)	aluminum
3	3	1/4	1/2	3/8 laminate (0.060 PVB)	aluminum
4	4	3/16	1/2	1/4	aluminum
5	1	1/8	-	-	steel
	1	5/32	-	-	steel
	1	3/16	-	-	steel
	1	1/4	-	-	steel

* laminates composed of 2 lites of glass

Table 2. Shock Tube Test Comparison of Monolithic Glass

Test No.	Glass Thickness (in)	Testing: Glass Break Time (ms)	Testing: Max. Defl. (in)	SBEDS-W Predictions: Glass Break Time (ms)	SBEDS-W Predictions: Max. Defl. (in)
1	1/4	7.7[1,2] ± 1	2.14 - 2.45[a]	no break	2.33
2	3/16	no break	1.42[a]	no break	1.54
3	3/16	break	1.92[a]	no break	2.67
8	1/4	5.3[1,2] ± 1	2.71 - 6.10[a]	4.15	2.98
16	1/8	5.5[1] ± 0.5	1.67 - 3.08[a]	5.17	2.82
17	5/32	6[1] ± 0.5	2.23 - 4.40[a]	no break	2.81
18	1/4	5[1] ± 0.5	1.03 - 3.58[a]	4.94	2.99

Notes: [1]ABS Estimation; [2]high-Speed Video Estimation
[a]Laser Deflection

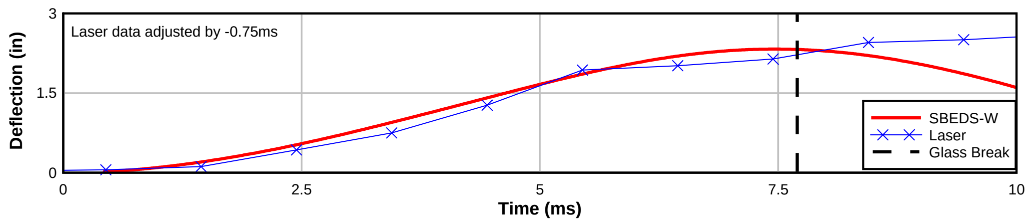

Figure 3. Shock Tube Test 1 Results: Deflection Comparison

In addition to the monolithic glass tests, several laminated IGU layups were tested. The shock tube pressure capacity was the limiting factor on the thicker glass layups (Type 2 and 3 as shown in Table 1) as higher pressures were needed to break the glass without subsequent over loading of the PVB. Higher impulses with lower pressures could be achieved to break the glass, but this resulted in a lack of control in the testing and caused PVB failure and catastrophic failure of the system, immediately after glass break occurred. Several successful and controlled tests were conducted, however. Table 3 shows the inner lite test results and the corresponding SBEDS-W predictions using an *m* of 6.4. On average, SBEDS-W predictions were 3% lower than the measured deflections of the inner lite when the glass did not break. However, the GFPM predicted no failure for each of the tests where the glass failed, suggesting that improvements could be made. The test data suggested that an adjusted value of *m* of 6.55 would account for these differences and provide better predictions for subsequent blast tests.

Table 3. Shock Tube Results: Laminated IGU Comparison

Test No.	Window Type	Testing: Glass Break Time (ms)	Testing: Max. Defl. (in)	SBEDS-W Predictions: Glass Break Time (ms)	SBEDS-W Predictions: Max. Defl. (in)	SBEDS-W Error (%)
9	1	6.1[2] ± 0.15	2.67[b]	no break	2.77	3.7%
10	1	7.2[2] ± 0.15	2.40[b]	no break	2.5	4.2%
11	1	no break	2.37[a]	no break	2.23	-5.9%
12	1	no break	2.55[b]	no break	2.42	-5.1%
13	1	6.2[2] ± 0.15	2.44[b]	no break	2.76	13.1%
14	3	no break	2.51[b]	no break	2.45	-2.4%
15	3	<6.7[2] ± 0.5	N/M	no break	2.9	N/M
19	2	no break	2.58[a]	no break	2.58	0.0%
20	2	no break	2.60[a]	no break	2.58	-0.8%
21	2	no break	2.77[a]	no break	2.66	-4.0%

Notes: [2]High-Speed Video Estimation
[a]Laser Deflection; [b]DIC Deflection; N/M - not measured

3.2 Blast Testing

Two full-scale blast tests were performed on twelve window assemblies (six per test) at the AFRL test facilities located on Tyndall Air Force Base in Panama City, Florida. Test 1 was performed on August 22, 2012 and Test 2 was performed on October 3, 2012 (Figure 4). Both tests were performed to validate the performance of IGUs incorporating Herculite® XP glass in punched window and storefront configurations using commercially available window frames.

PEC performed analysis with measured loads and response data to compare with results from the models. SDOF analyses were performed using SBEDS-W. The SBEDS-W glass module was calibrated to match results from the previously conducted static tests and shock tube tests with model values of m = 6.55, k = 2.86×10^{-53} $N^{-7}m^{12}$, POF = 500, and LF = 1. The predicted and observed response of each IGU is summarized in Table 4 (note, predictions were made assuming a single window with rigid supports). In all cases, the SBEDS-W glazing response predictions are conservative as was expected given the assumption of rigid supports.

Figure 4. Blast Test 2 Results

Table 4. Blast Test Comparison

Test No.	Bay	Window Type	Layup Type	Glazing Response		Max. Disp. (in)	
				Observed	Predicted[1]	Measured[2]	Predicted[1]
1	1	Storefront	4	no break	fail glass	2.96	-
	2	Storefront	2	no break	no break	3.16	1.7
	3	Punched	1	break[3,4]	break[3]	7.9	2.3
	4	Storefront	1	no break	break[3]	3.46	2.3
	5	Punched	4	fail glass	fail glass	-	-
		Punched	1	break[4]	fail pvb	-	-
	6	Punched	4	fail glass	fail glass	-	-
		Punched	4	fail glass	fail glass	-	-
2	1	Storefront	3	break[3]	break[4]	-	2.3
	2	Storefront	(3) 3 & (1) 2	break[3,4]	break[4]	-	7.6
	3	Punched	3	break[4]	break[4]	6.04	7.6
	4	Storefront	1	break[4]	fail pvb	13.56	-
	5	Punched	4	fail glass	fail glass	-	-
		Punched	1	fail pvb	fail pvb	-	-
	6	Punched	4	fail glass	fail glass	-	-
		Punched	4	fail glass	fail glass	-	-

[1] predictions made with SBEDS-W using m = 6.55

[2] measured data is from laser gauges prior to rigid body motion of the frame

[3] outer lite break, inner lite not break

[4] PVB activated and stretched

4. Data Analysis of Deformed Shape

4.1 Digital Image Correlation

Response of the glass and mullions was measured using the 3D DIC method. DIC can make thousands of measurements over the entire visible area of the system thereby providing a full surface representation of deformation in time than is possible and/or practical with traditional deflection measurement approaches. This measurement technique uniquely facilitates detailed analysis of the deformed shape of the glazing and mullions and their interaction. Deformed shape is typically assumed to remain parabolic for glazing and mullions over the full history of response. In reality, deformed shape changes in time, significantly altering assumptions of inertial resistance in the predictive models. DIC can also be used to further develop multi degree of freedom (MDOF) or finite element analysis (FEA) models for coupled glazing and mullion system response that incorporate information learned from the deformed shape analysis.

2D and 3D DIC has been used in a number of industries for at least the past 10 years mainly for the measurement and depiction of strain fields as they develop in material specimens or structural components undergoing static testing. The accuracy and reliability of 3D DIC measurements are dependent solely on the quality of the images captured by the stereoscopically mounted cameras. With the recent development of reasonably priced, high speed, high resolution digital cameras (2-4M pixels) over the past 3-5 years, the number of potential applications of this technology has also grown to include dynamic testing. AFRL has since developed specialized implementation techniques that now allow for accurate and reliable 3D DIC measurements in laboratory and full scale air blast environments.

This data from the shock tube and blast tests allowed PEC to verify the deformed shape of the window during dynamic response, analyse strain (and stress) concentrations for FEA validation, and monitor frame movement during the window response. The deformed shape of the glazing and mullions is used for validation of FEA and can be used to determine the load-mass factors in SDOF analysis. In the shock tube tests, only the deflection of the glazing was measured; therefore the deflection of the mullions can only be inferred based on extrapolation from glazing deflection. However, in the blast tests, the mullion response was measured and can be used to analyse the interaction between the glazing and mullions. The coupled effects of the interaction between the mullions and the glazing during dynamic response are discussed further in Alberson et al (2013).

4.2 Glazing Deformed Shape

The deformed shape of the glazing observed from the DIC during the shock tube testing shows that a parabolic deformed shape occurs after inertial effects and a flat plate type of response have been overcome early in the response as shown in Figure 5. Each line represents the deformed shape at a single point in time for the horizontal cross section of the glazing at an interval of 0.153ms. The middle section of the glass is not stressed initially and responds more as a rigid body mass than a plate in flexure. However, the stress incrementally works towards the centre of the window until all glass is contributing to resistance of the load through bending. At this point in time the glazing behaves according to plate theory and the deformed shape becomes roughly parabolic. This is the assumed deformed shape for the load-mass factors associated with SDOF calculations.

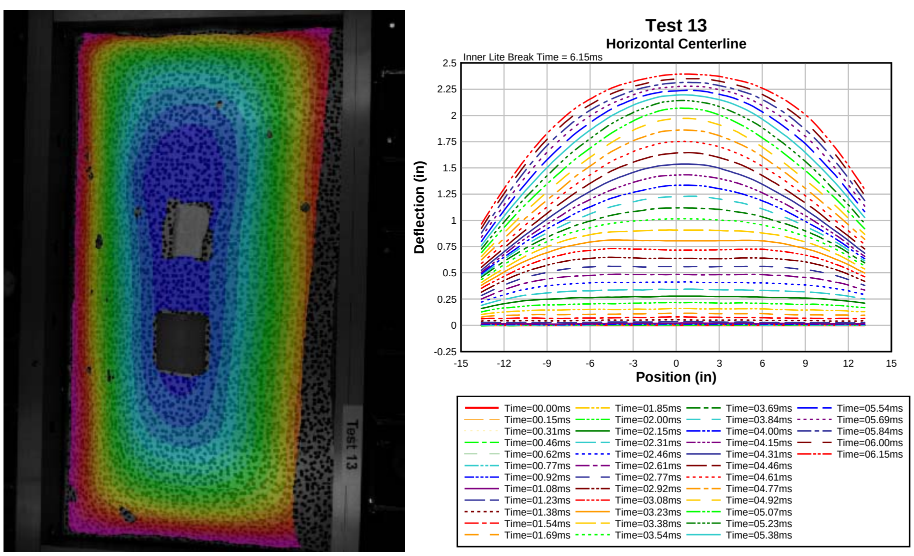

Figure 5. (left) DIC Deflection Contours overlaid on the High-Speed Video and (right) Vertical Centerline Deflection History up to Laminated Inner Lite Failure.

For the size and strength of windows tested in this program, the glazing is capable of withstanding the load long enough to transition into large displacement plate response, which explains the good pre-test predictions from SDOF analysis. With this in mind, the analysis was able to accurately predict the response of the glazing based on plate theory and the failure criteria specified through the modified GFPM. However, for larger or different aspect ratio windows or for different strength glass this may not be true. More work is needed to investigate this phenomena; one possible path forward is to look at the use of a stress based implementation of the GFPM in FEA rather than the deflection based implementation used in ASTM E1300.

After the glass failed, the DIC data continued to define the response of the glazing through the PVB response phase (Figure 6). Notice the larger deflection of the top and bottom (left and right of the plot) of the glazing compared to the centre of the glazing. The material in the top and bottom of the window is moving faster than the material at the centre of the glass. This was also seen on tests with monolithic lites where the glass debris was monitored and tracked. Regardless of whether the glazing is monolithic or laminated, the tests illustrated that the material that fractures first has the highest velocity after fracture.

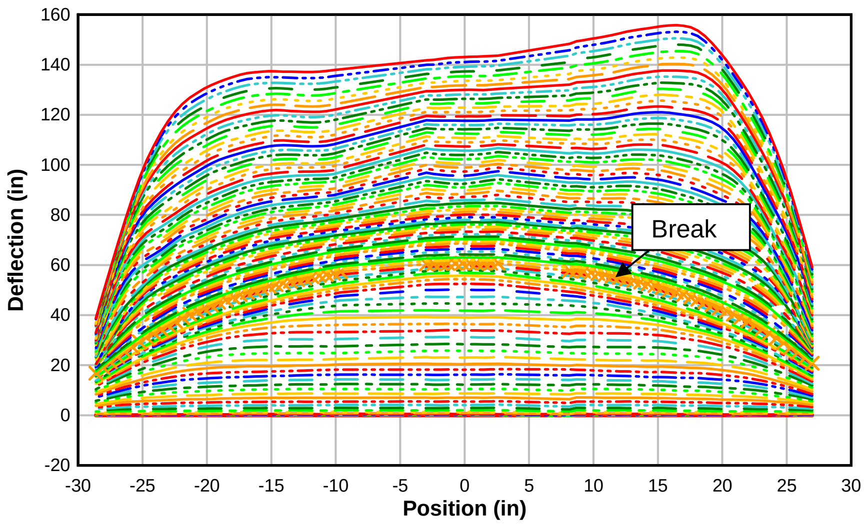

Figure 6. Shock Tube Test 13 Vertical Centerline Deflection History – Laminate.

This could be due to energy release from glass fracture or elastic rebound from the unfractured glass. The glass first cracks in the corners, where the stress is the highest (discussed further in the FEA validation section). As the glass fractures, the stored energy in the glass (due to bending and tempering) is released starting in the corners. The effects of the fracture in the corners are two-fold; the energy release propels the fractured glass and the unfractured glass as the centre begins to relieve the bending stress by returning to a flat plate. This all takes place over the course of ~1ms, but this appears to be enough time for the centre of the window to act as an anchor while the edges (where the cracks initiated) accelerate. If this is true, it indicates that the stress relief runs just ahead of the crack propagation. Further FEA and test data are needed to validate this assessment of the observed test data.

If the glazing is laminated, the glass will accelerate until the PVB forms a tension membrane to further resist the load. Again, the deformed shape of the PVB in tension membrane does not occur immediately at the time of glass fracture, but forms gradually. It starts at the edges and moves towards the centre similar to the formation of the deformed shape during the glass dominated response phase.

By differentiating the DIC data, the velocity profile of the glass debris can be analysed. This is useful, along with debris size, in predicting shard fly-out characteristics, which ultimately correspond to injury potential. Coupled with debris size and mass distribution data from the debris fly-out analysis, this data was used to further calibrate debris fly-out models and to link the results to injury potential.

4.3 FEA Validation through Strain Analysis

The immense amount of data on the deflected shape of the glazing allows the slope of the deflected shape and the glass strains to be calculated and compared to the simulation. Figure 8 and Figure 9 show a comparison between DIC and FEA of the deflection and 1^{st} principal stress, respectively. The stress calculation was based on Hooke's law assumptions and is thus directly proportional to the measured strain.

The fringes shown in Figure 8 are for the same point in time (at maximum deflection). Notice the good correlation on the magnitude of deflection and contour shape in Figure 8 and the stress concentrations in the corners of the glazing in Figure 9. Also, notice the difference in the amount of stress shown in the middle of the glazing. FEA provides the complete surface and through thickness theoretical stress state of the elements in this region which can be compared to the stress state calculated from DIC deflection measurements at the surface of the glass. The measurements are manipulated into surface strains by calculating the change in distance between the points over time. The strain to stress transform is straightforward for pure bending or pure tension situations. However, as the boundary conditions on the glazing start to produce tension through the cross section, and the assumptions of pure bending begin to add the effects of tension membrane, the strain distribution is harder to identify. To estimate the strain distribution, the curvature (2nd derivative of the deflection profile) was used to attempt to quantify local bending in the vertical and horizontal direction. This method shows promise, but more work is needed to further investigate the capability of measuring the strain distribution through the thickness of the glazing and accurately calculate the stress at any given point.

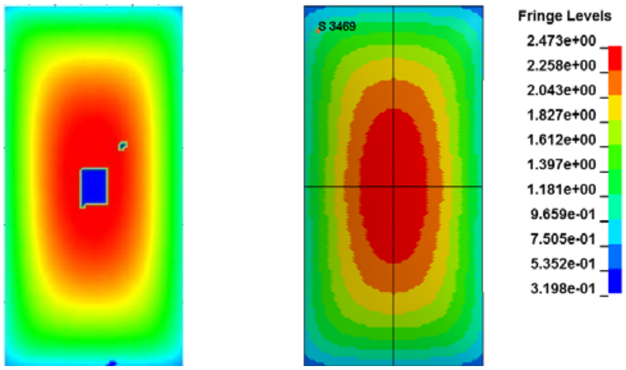

Figure 8. Deflection Comparison of (left) DIC and (right) FEA.

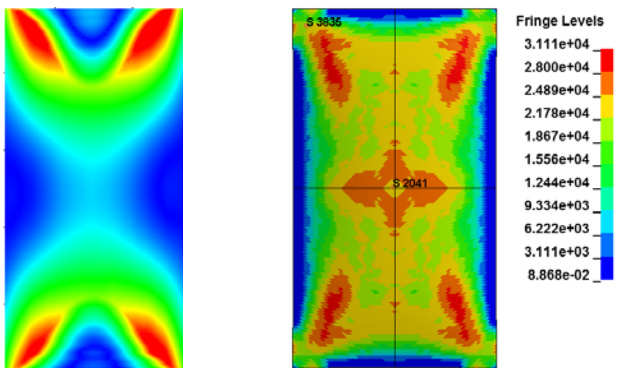

Figure 9. 1st Principal Stress Comparison at Maximum Deflection of (left) DIC and (right) FEA.

5. Conclusions

The test program provided sufficient data to evaluate a resistance function for IGUs containing Herculite® XP glass for use in a SDOF analysis program. Comparisons with test data illustrate that the model can conservatively predict the performance of IGUs containing Herculite® XP glass subjected to shock loads.

Shock tube and blast testing showed good correlation with SDOF predictions made with SBEDS-W based on consistent and conservative glazing failure predictions. Additionally, the resistance curve generation based on the polynomial method found in Appendix X2 in ASTM E1300 was verified with the static test results.

Deformed shape assumptions for the glazing and the mullions can be measured in dynamic load scenarios to capture the deformed shape of the system and each component individually. The deformed shape can be used to identify the mechanics of the material during response, and can allow calculation of strain and stress distribution during elastic and plastic response, and material failure. The deformed shape of the glass is consistent with large deformation plate theory and exhibits a parabolic shape soon after load is applied, and more importantly, during the time of fracture. Therefore, the load-mass factors used to idealize the deformed shape of the glazing for SDOF analysis appear to provide accurate and conservative results for the high strength glass tested in this project.

Acknowledgements

The authors would like to acknowledge the contributions and guidance from the PEC internal team and the efforts of external subcontractors and associates. The research reported herein was conducted as part of the Defense Acquisition Challenge (DAC) program for the Air Force Research Laboratory, Airbase Technologies Division, Tyndall Air Force Base, FL (AFRL). PPG Industries, Inc. and Physical Security,

LLC provided the glazing and mullions, respectively. Shock tube and blast testing was performed by ABS Consulting and AFRL, respectively.

References

[1] Alberson RM, Davis CE, Marchand KA, Conrath EJ, and Misko SR (2013) Deformed Shape Analysis of Coupled Glazing. In Proceedings of 15 ISIEMS Conference in Potsdam, Germany.

[2] Beason WL and Morgan JR (1984) Glass Failure Prediction Model. Journal of Structural Engineering. Vol. 110, No. 2. ASCE, Feb.

[3] ASTM Standard E1300 (2012) Standard Practice for Determining Load Resistance of Glass in Buildings. ASTM International, West Conshohocken, PA. USA, DOI: 10.1520/F2248-09. www.astm.org.

[4] Morse SM and Norville HS (2012) Design Methodology for Determining the Load Resistance of Heat-Treated Window Glass. Journal of Architectural Engineering. Vol. 18, No. 1. ASCE, Mar.

[5] Vallabahn CVG and Wang BYT (1981) Nonlinear Analysis of Rectangular Glass Plates by Finite Difference Method. Institute for Disaster Research, Texas Tech University. Lubbock, Texas: Jun.

[6] US Army Corps of Engineers Protective Design Center (2012) Single degree of freedom Blast Effects Design Spreadsheet for Windows Version 1.0 (SBEDS-W). Dec.